

State-of-the-Art CT Technology and a Glimpse into the Future

Marc Kachelrieß

German Cancer Research Center (DKFZ)

Heidelberg, Germany

www.dkfz.de/ct

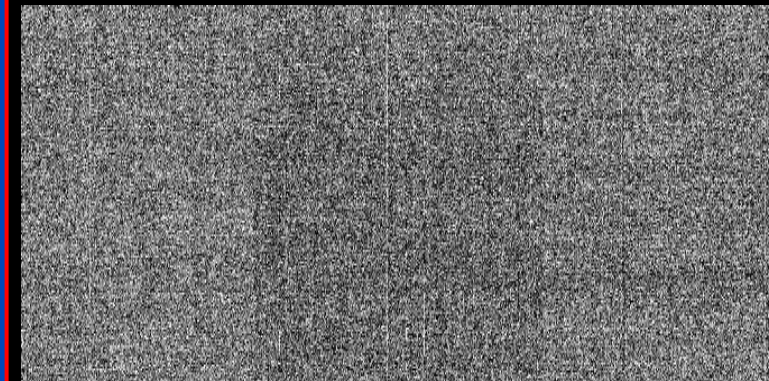


DEUTSCHES
KREBSFORSCHUNGSZENTRUM
IN DER HELMHOLTZ-GEMEINSCHAFT

Advantages of Photon-Counting CT

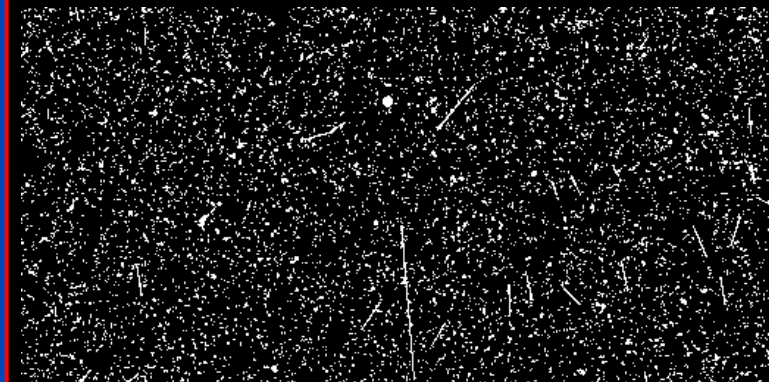
- **No reflective gaps between detector pixels**
 - Higher geometrical efficiency
 - Less dose
- **No electronic noise (every photon counts)**
 - Less dose for infants
 - Less noise for obese patients
- **Counting**
 - Swank factor = 1 = maximal
 - “Iodine effect“ due to higher weights on low energies
- **Energy bin weighting**
 - Lower dose/noise
 - Improved iodine CNR
- **Smaller pixels (to avoid pileup)**
 - Higher spatial resolution
 - “Small pixel effect” i.e. lower dose/noise at conventional resolution
- **Spectral information on demand**
 - Dual Energy CT (DECT), Multi Energy CT (MECT)
 - Standardization (e.g. VMI)

EI (Dexela)



Readout noise only. Single events hidden!

PC (Dectris)

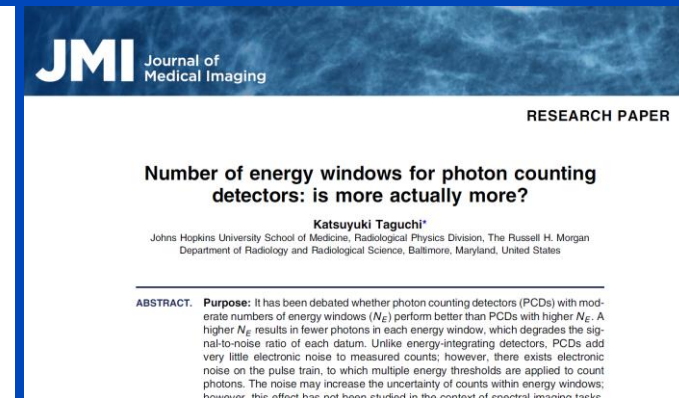
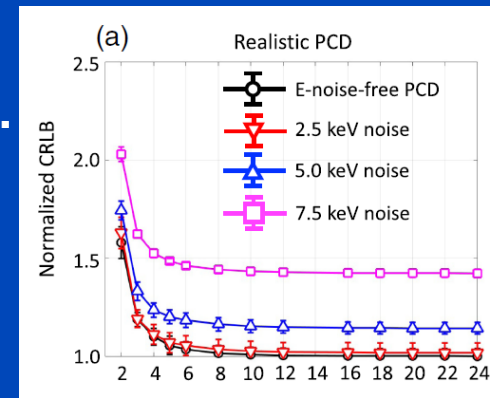


No readout noise. Single events visible!

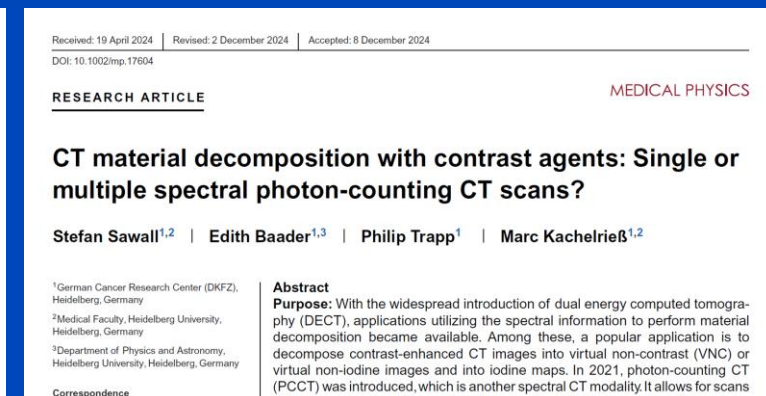
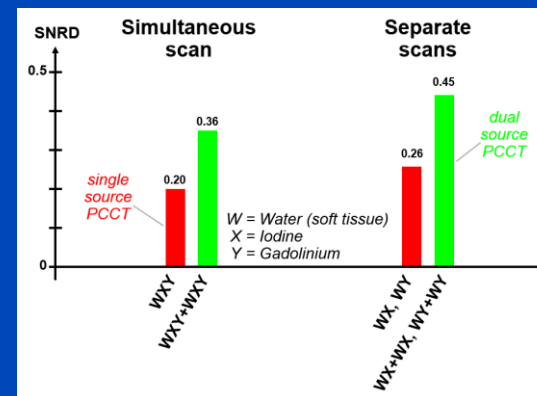
18 frames, 5 min integration time per frame, x-ray off

Do We Want Many Energy Bins? Do We Want Multi-Contrast Imaging?

- How many bins do we need?
 - For M materials we need at least $B = M$ energy bins.
 - Little more, e.g. $M+2$, may help to reduce noise.
 - 2 materials are abundant in patients (no k-edges)
 - 3 materials in patients with k-edge contrast agent
 - Warning: k-edge of iodine is very low (33 keV)



- Is it good to simultaneously inject two contrast agents to increase M if one could get the same result from two separate scans?
 - Definitely not^{1, 2, 3}
 - Noise will increase stronger than if one had distributed the imaging dose into two separate CT scans³.



¹Ren et al. Radiation dose efficiency of multi-energy photon-counting-detector CT for dual-contrast imaging. Phys. Med. Biol. 64(24): 245003 (13pp), 2019.
²Ren et al. Quantitative accuracy and dose efficiency of dual-contrast imaging using dual-energy CT: A phantom study, Med. Phys. 47(2): 441–456, 2020.
³Sawall, Kachelrieß et al. CT material decomposition with contrast agents: Single or multiple spectral photon-counting CT scans? A simulation study. Med. Phys. 52, 2025.

Content

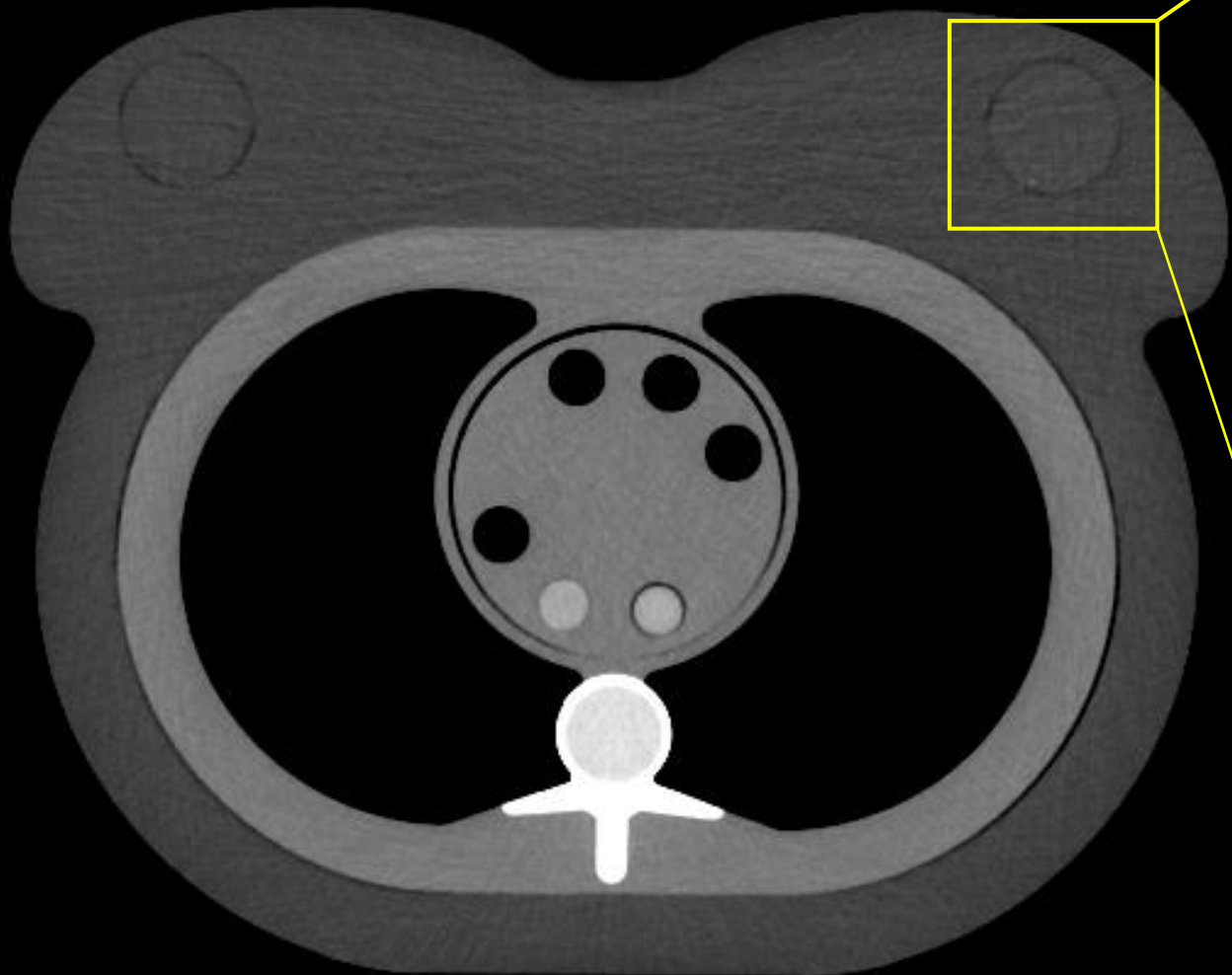
- Opportunistic screening
- Patient-specific prefilters
- Small pixel effect
- X-ray target design
- riskTCM

Incidental Findings

OPPORTUNISTIC SCREENING

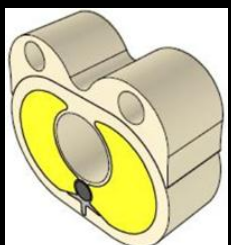
Screening and Opportunistic Screening

- **Screening becomes more and more attractive with PCCT due to**
 - Higher spatial resolution
 - Lower radiation dose
 - Standardized CT values
 - Better image quality
- **Screening and opportunistic screening options under discussion**
 - Lung cancer screening (national screening programs partially available)
 - Coronary artery calcification scoring, CACS
 - Breast cancer screening
 - Osteoporosis screening
 - Body composition
 - ...



22 mm

Naeotom Alpha.Peak, 120 kV, 20 mGy CTDI_{32 cm},
 Br40 kernel, QIR(3), pixel size 0.73 mm,
 slice thickness 2.5 mm, slice increment 1.0 mm,
 C = 40 HU, W = 400 HU



Structures in the Inserts (measured with thorax)

	Calcifications	Fibers	Masses (100 HU contrast)
0.40 mm		0.60 mm	6.32 mm
0.29 mm		0.41 mm	4.67 mm
0.20 mm		0.23 mm	3.18 mm
0.13 mm		0.15 mm	1.8 mm

6 mm

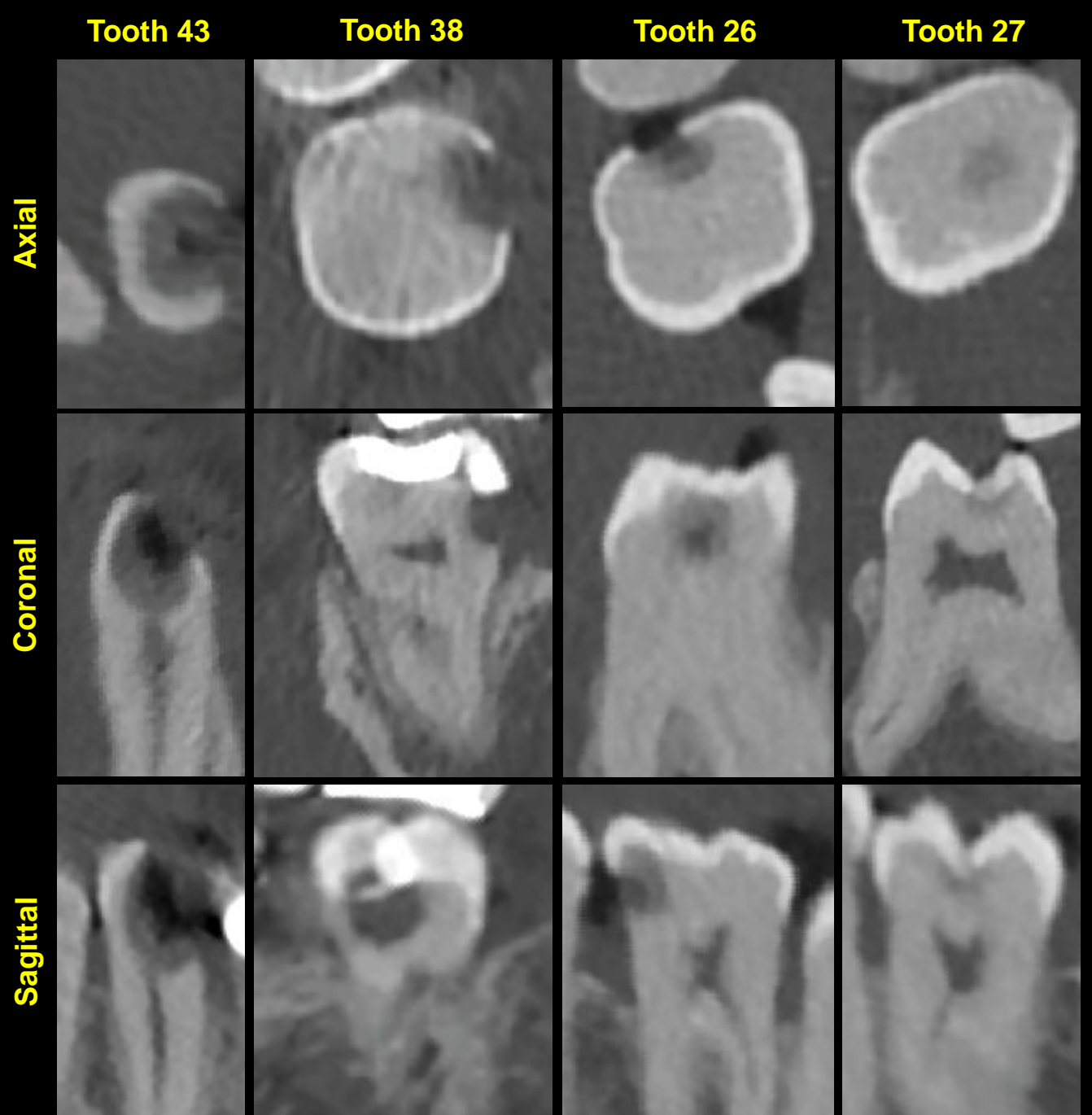
Naeotom Alpha.Peak, 120 kV, 20 mGy CTDI_{32 cm}, UHR,
 Br72 kernel, QIR(3), pixel size 0.097 mm,
 slice thickness 0.2 mm, slice increment 0.1 mm,
 C = 40 HU, W = 400 HU

	BCT		PCCT (Naeotom Alpha)			
	7.0 mGy (CTDI _{16 cm})	7.0 mGy (CTDI _{16 cm})	1.3 mGy (CTDI _{32 cm})	3.5 mGy (CTDI _{32 cm})	7.1 mGy (CTDI _{32 cm})	12.5 mGy (CTDI _{32 cm})
0.13 mm						
0.20 mm						
0.29 mm						
0.40 mm						
	$D_{\text{eff}} = 0.84 \text{ mSv}$ $D_{\text{B}} = 7.00 \text{ mSv}$	$D_{\text{eff}} = 0.84 \text{ mSv}$ $D_{\text{B}} = 7.00 \text{ mSv}$	$D_{\text{eff}} = 0.73 \text{ mSv}$ $D_{\text{B}} = 1.40 \text{ mSv}$	$D_{\text{eff}} = 1.96 \text{ mSv}$ $D_{\text{B}} = 3.76 \text{ mSv}$	$D_{\text{eff}} = 3.98 \text{ mSv}$ $D_{\text{B}} = 7.63 \text{ mSv}$	$D_{\text{eff}} = 7.00 \text{ mSv}$ $D_{\text{B}} = 13.42 \text{ mSv}$
	Breast Phantom Only		Breast and Thorax Phantom			

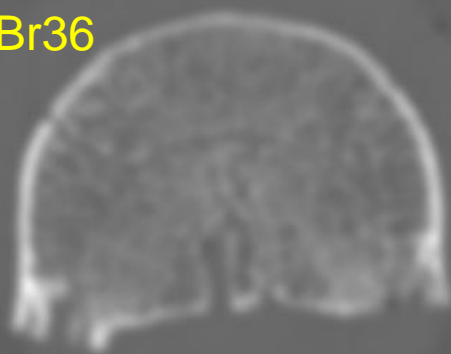
CTDI_{16 cm}
 \approx
2.1 CTDI_{32 cm}

Opportunistic Diagnosis of Carious Defects in Routine Head and Neck Scans

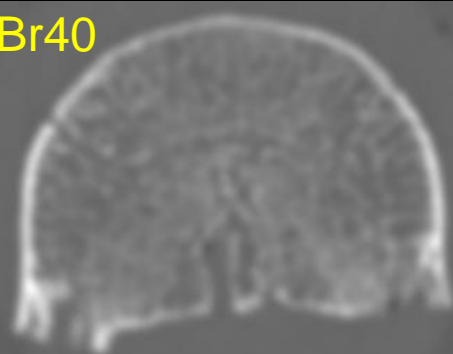
- Naeotom Alpha.Peak
- Br72
- $CTDI_{32\text{ cm}} = 13\text{ mGy}$
- $C = 1300\text{ HU}$, $W = 6000\text{ HU}$



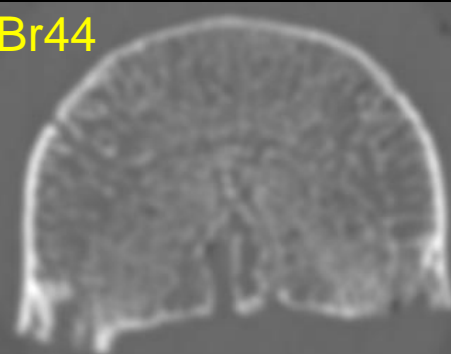
Br36



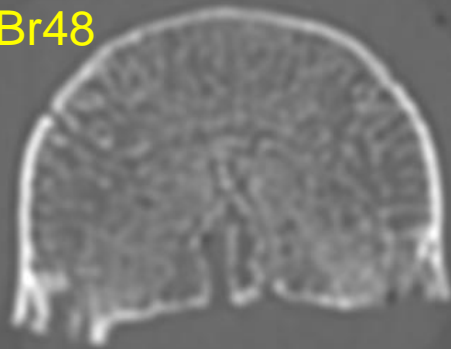
Br40



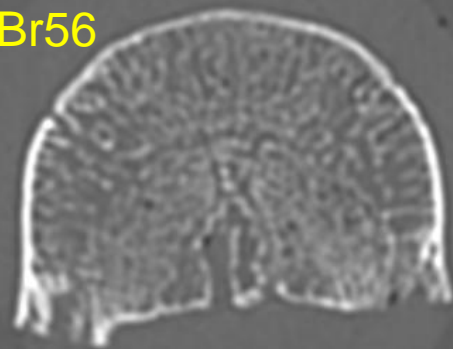
Br44



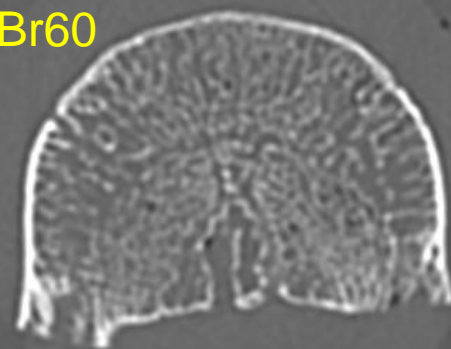
Br48



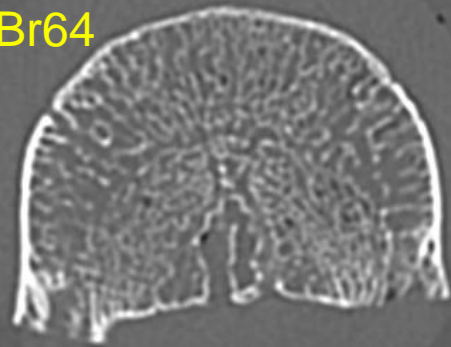
Br56



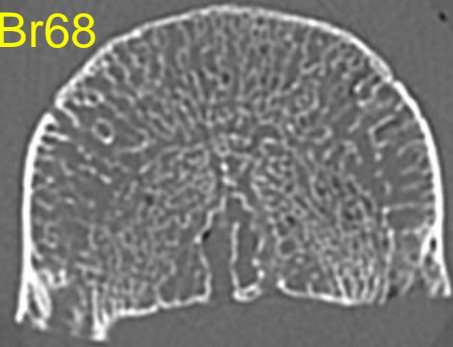
Br60



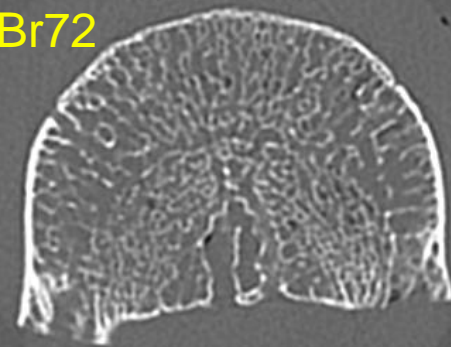
Br64



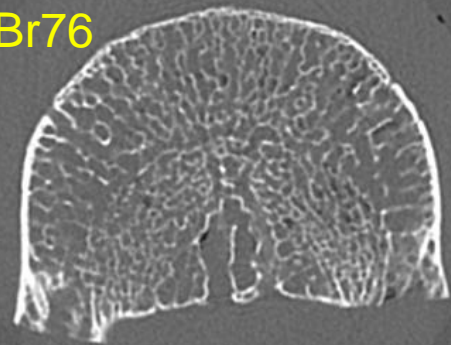
Br68



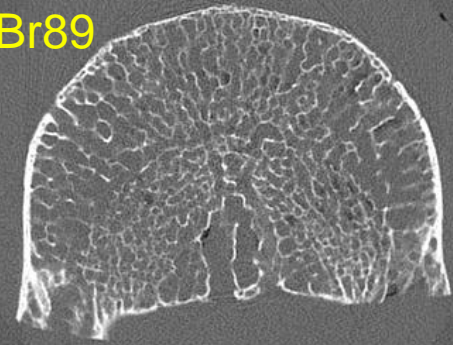
Br72



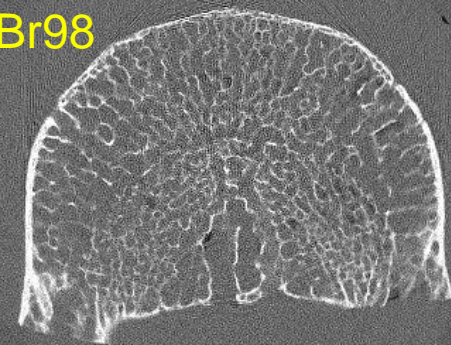
Br76



Br89



Br98



} \approx EI

Vertebra at
Naeotom
Alpha.Peak in
UHR mode.

C = 500 HU
W = 3000 HU

4 cm



PATIENT-SPECIFIC PREFILTRATION

Siemens Naeotom Alpha.Peak

The World's First Photon-Counting CT

- **Tubes**

- tube A: 120 kW
 - tube B: 120 kW
- } $\approx \frac{1}{4}$ MW
- Focal spot size down to 181 μm

- **Detectors**

- pixel size down to 150 μm
- 288 detector rows
- 2752 detector columns

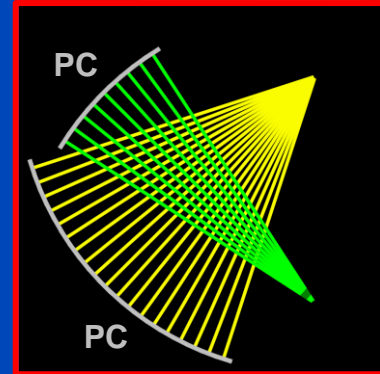
- **Speed**

- up to 4 rotations per second
- up to 737 mm/s scan speed
- down to 66 ms native temporal resolution

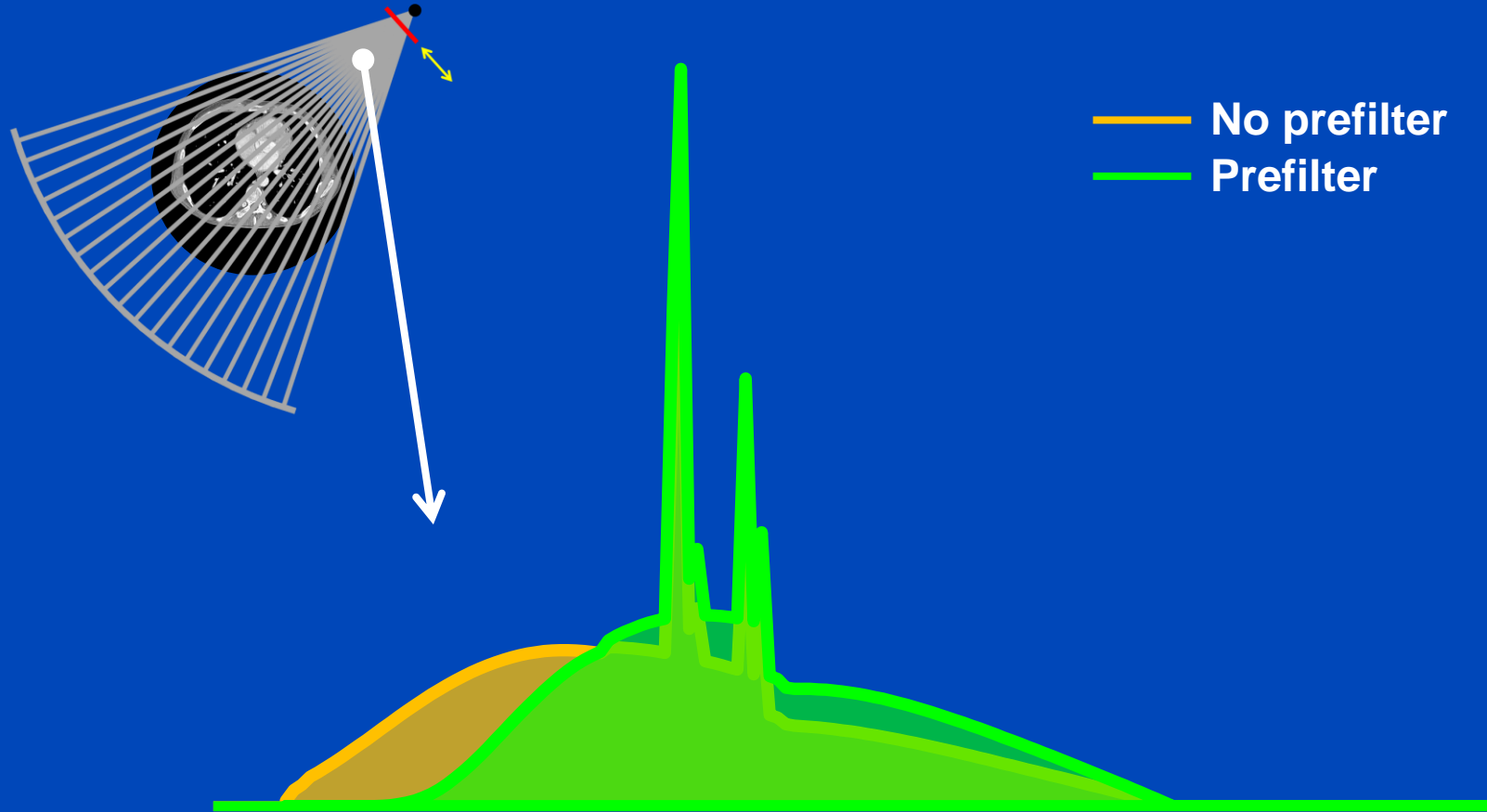
- **50 cm FOM**

- **Spectral**

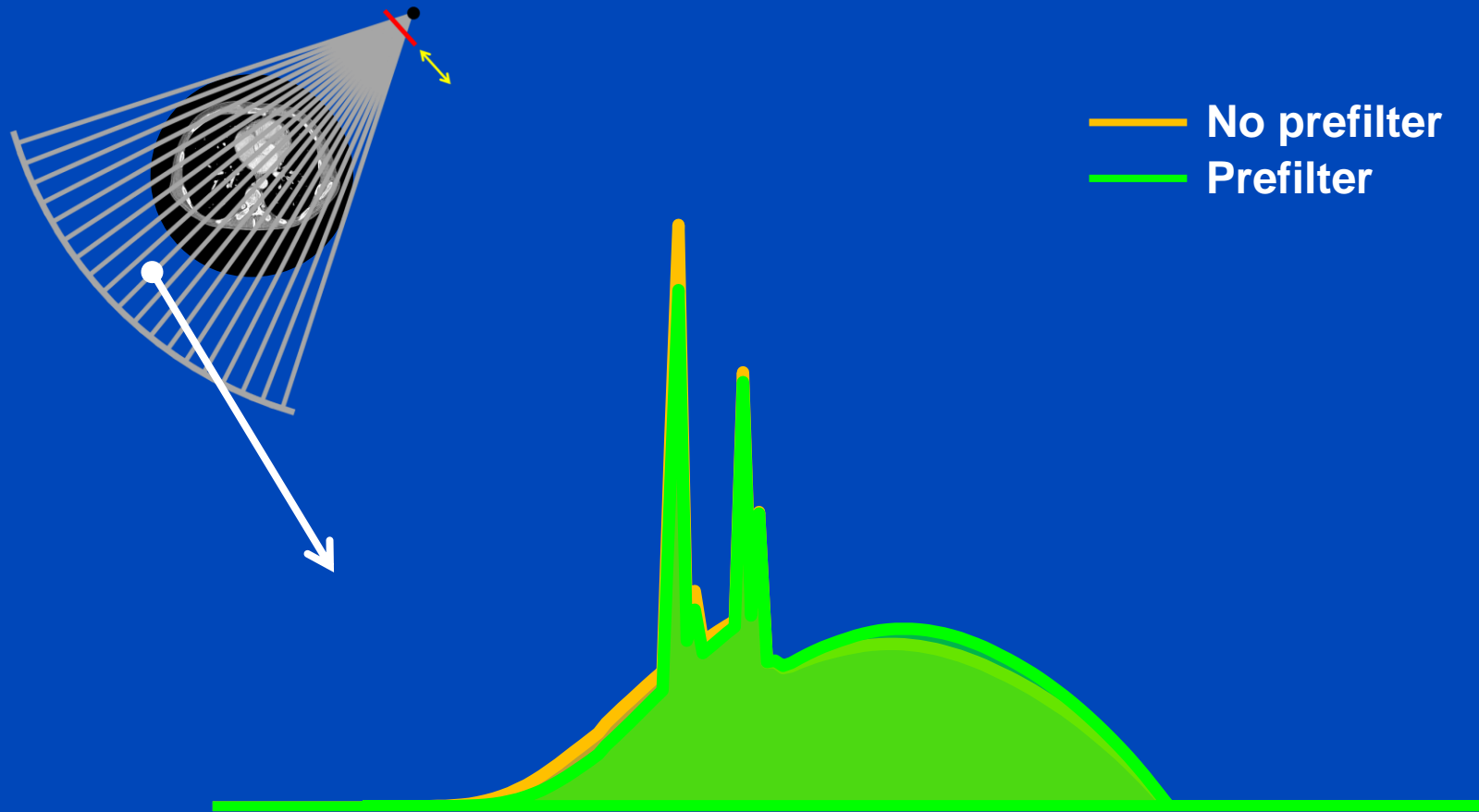
- VNC, VNCa (pure lumen), VMI
- Z_{eff} , electron density, ...



120 kV + 0 mm water with and without prefilter



120 kV + 320 mm water with and without prefilter



Task- and Patient-Specific, i.e. Removable, Prefilters in Use Today

- 0.4 mm Sn for Siemens` Naeotom Alpha.Prime and Alpha.Pro
- 0.4 mm and 0.7 mm Sn for Siemens` Naeotom Alpha.Peak and Alpha.Pro
- 0.6 mm Sn for Siemens` Somatom Force, Edge Plus, go.Top and Definition Edge
- 0.4 mm Sn for Siemens` Somatom Flash, Drive, go.Now, go.Up, go.all, and pro.Pulse
- 0.4 mm and 0.7 mm Sn for Siemens` Somatom X.cite
- ≈ 0.5 mm Au for Canon`s Aquilion ONE Prism Edition
- ≈ 1 mm Cu “for scout scans” in GE`s Revolution Apex systems

In the energy range of clinical CT and with objects similar to patients we find that **0.5 mm Ag \approx 0.6 mm Sn \approx 2.0 mm Cu.**

Dose Reduction due to Tin Prefiltration

Reference	Topic	Dose Reduction	Assessment	Recon
Agostini et al., 2021	chest, DECT, COVID-19	89%	subjective, different pitch values	iterative
Apfaltrer et al., 2018	coronary artery calcium scoring	73%	subjective	FBP
Axer et al., 2022	urolithiasis	20%	subjective	iterative
Dewes et al., 2016	abdomen, urinary stones	22%	subjective	iterative
Gordic et al., 2014	chest, pulmonary nodules, phantom	95%	subjective	iterative
Grunz et al., 2022	urinary stone	18% - 38%	subjective, objective	iterative
Hasegawa et al., 2022	chest, detectability index, phantom	22% - 25%	objective	FBP
Jeon et al., 2019	DECT, gout diagnosis	65%	subjective, different scanners	iterative
Kimura et al., 2022	colorectal cancer	89%	subjective	iterative, FBP
Kunz et al., 2022	urinary tract	62%	frequency of calculi detection	iterative
Leyendecker et al., 2019	abdomen	81%	subjective, objective	iterative
Martini et al., 2016	chest, pulmonary nodules	97%	subjective	iterative
Rajendran et al., 2020	sinus, temporal bone	67% - 85%	objective, EICT and PCCT	FBP
Saltybaeva et al., 2019	topogram	80%	effect on TCM	-
Schabel et al., 2018	thoracic aorta calcification	92%	subjective	iterative
Schüle et al., 2022	pelvis	90%	subjective, objective	iterative, FBP
Takemitsu et al., 2022	topogram	80%	effect on TCM	-
Weis et al., 2017	chest, pediatric	77%	subjective, objective	iterative
Wuest et al., 2016	paranasal sinus	73%	subjective, different scanners	FBP
Zhang et al., 2022	guided lung biopsy	73%	subjective	iterative

Dose Reduction due to Tin Prefiltration

1. Agostini, Andrea, et al. "Third-generation iterative reconstruction on a dual-source, high-pitch, low-dose chest CT protocol with tin filter for spectral shaping at 100 kV: a study on a small series of COVID-19 patients." *La radiologia medica* 126:388–398, 2021.
2. Apfaltrer, Georg, et al. "High-pitch low-voltage CT coronary artery calcium scoring with tin filtration: accuracy and radiation dose reduction." *European Radiology* 28(7):3097-3104, 2018.
3. Axer, Benedikt, et al. "Comparative evaluation of diagnostic quality in native low-dose CT without and with spectral shaping employing a tin filter in urolithiasis with implanted ureteral stent." *RöFo-Fortschritte auf dem Gebiet der Röntgenstrahlen und der bildgebenden Verfahren* 194(12):1358-1366, 2022.
4. Dewes, Patricia, et al. "Low-dose abdominal computed tomography for detection of urinary stone disease - Impact of additional spectral shaping of the x-ray beam on image quality and dose parameters." *European Journal of Radiology* 85(6):1058-1062, 2016.
5. Gordic, Sonja, et al. "Ultralow-dose chest computed tomography for pulmonary nodule detection: First performance evaluation of single energy scanning with spectral shaping." *Investigative Radiology* 49(7):465-473, 2014.
6. Grunz, Jan-Peter, et al. "Thermoluminescence dosimetry in abdominal CT for urinary stone detection: Effective radiation dose reduction with tin prefiltration at 100 kVp." *Investigative Radiology* 58(3):231-238, 2023.
7. Hasegawa, Akira, et al. "A tin filter's dose reduction effect revisited: Using the detectability index in low-dose computed tomography for the chest." *Physica Medica* 99:61-67, 2022.
8. Jeon, Ji Young, et al. "The effect of tube voltage combination on image artefact and radiation dose in dual-source dual-energy CT: Comparison between conventional 80/140 kV and 80/150 kV plus tin filter for gout protocol." *European Radiology* 29(3):1248-1257, 2019.
9. Kimura, Koichiro, et al. "Dose reduction and diagnostic performance of tin filter-based spectral shaping CT in patients with colorectal cancer." *Tomography* 8(2):1079-1089, 2022.
10. Kunz, Andreas Steven, et al. "Tin-filtered 100 kV ultra-low-dose abdominal CT for calculi detection in the urinary tract: A comparative study of 510 cases." *Academic Radiology*, 2022.
11. Leyendecker, Pierre, et al. "Prospective evaluation of ultra-low-dose contrast-enhanced 100-kV abdominal computed tomography with tin filter: effect on radiation dose reduction and image quality with a third-generation dual-source CT system." *European Radiology* 29(4):2107-2116, 2019.
12. Martini, Katharina, et al. "Evaluation of pulmonary nodules and infection on chest CT with radiation dose equivalent to chest radiography: Prospective intra-individual comparison study to standard dose CT." *European Journal of Radiology* 85(2):360-365, 2016.
13. Rajendran, Kishore, et al. "Dose reduction for sinus and temporal bone imaging using photon-counting detector CT with an additional tin filter." *Investigative Radiology* 55(2):91-100, 2020.
14. Saltybaeva, Natalia, et al. "Radiation dose reduction from computed tomography localizer radiographs using a tin spectral shaping filter." *Medical Physics* 46(2):544-549, 2019.
15. Schabel, Christoph, et al. "Tin-filtered low-dose chest CT to quantify macroscopic calcification burden of the thoracic aorta." *European Radiology* 28:1818-1825, 2018.
16. Schüle, Simone, et al. "Low-dose CT imaging of the pelvis in follow-up examinations-significant dose reduction and impact of tin filtration: Evaluation by phantom studies and first systematic retrospective patient analyses." *Investigative Radiology* 57(12):789-801, 2022.
17. Takemitsu, Masaki, et al. "Patient dose reduction for a localizer radiograph with an additional tin filter in chest-abdomen-pelvis, spine, and head computed tomography examinations." *Radiological Physics and Technology*, 2023.
18. Weis, Meike, et al. "Radiation dose comparison between 70 kVp and 100 kVp with spectral beam shaping for non-contrast-enhanced pediatric chest computed tomography: a prospective randomized controlled study." *Investigative Radiology* 52(3):155-162, 2017.
19. Wuest, Wolfgang, et al. "Low-dose CT of the paranasal sinuses: minimizing x-ray exposure with spectral shaping." *European Radiology* 26(11):4155-4161, 2016.
20. Zhang, Jing, et al. "Low-dose CT with tin filter combined with iterative metal artefact reduction for guiding lung biopsy." *Quantitative Imaging in Medicine and Surgery* 12(2):1359, 2022.
21. ... and many more ...

LUNG CANCER SCREENING CT (selected SIEMENS scanners, continued)[\(Back to INDEX\)](#)

TOPOGRAM: PA; scan from top of shoulder through mid-liver.

SIEMENS	Definition DS (Dual source 64-slice)	Somatom Drive (Dual source 128-slice)	Definition Flash (Dual source 128-slice)	Definition Force (Dual source 192-slice)
Software version	VA44	VB10	VB10	VB10
Scan Mode	Spiral	Spiral	Spiral	Spiral
Rotation Time (s)	0.5	0.5	0.5	0.5
Detector Configuration	*64 × 0.6 mm (32 × 0.6 mm = 19.2 mm)	*128 × 0.6 mm (64 × 0.6 mm = 38.4 mm)	*128 × 0.6 mm (64 × 0.6 mm = 38.4 mm)	*192 × 0.6 mm (96 × 0.6 mm = 57.6 mm)
Pitch	1.2	1.2	1.2	1.2
kV	120	100Sn (0.4 mm)	120	100Sn (0.6 mm)
Quality ref. mAs	20	81	20	101
CARE Dose4D	ON	ON	ON	ON
CARE kV	ON	ON	ON	ON
CTDIvol***	1.4 mGy	0.6mGy	1.3 mGy	0.4 mGy

RECON 1

Type	Axial	Axial	Axial	Axial
Kernel	B31f	Bf37, strength = 3**	Bf37, strength = 3**	Br40, strength = 3**
Slice (mm)	5.0	5.0	5.0	5.0
Increment (mm)	5.0	5.0	5.0	5.0

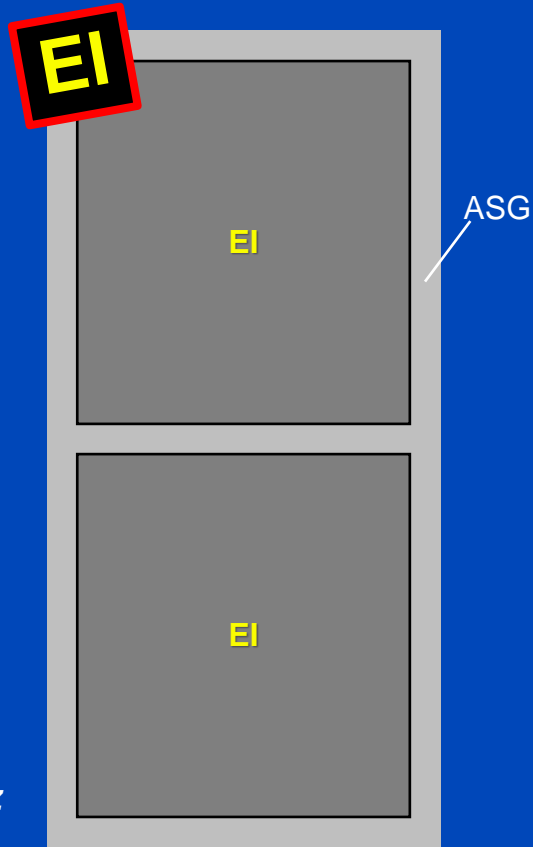
→ thicker prefilter means less dose

SMALL PIXEL EFFECT

Detector Pixel Force vs. Alpha

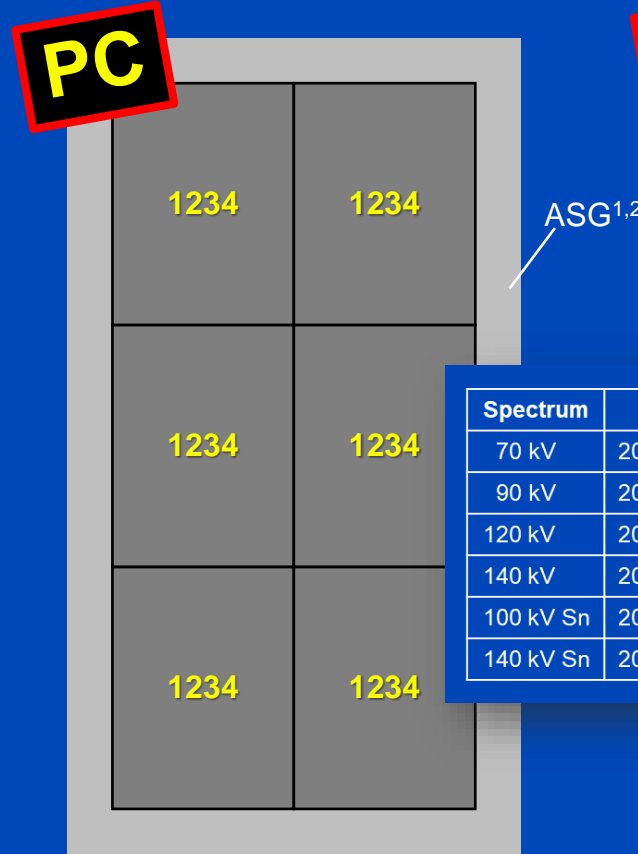
Force

920 × 96 detector pixels
 pixel size 0.52 × 0.56 mm at iso
 avg. sampling 0.56 × 0.6 mm at iso
 57.6 mm z-coverage



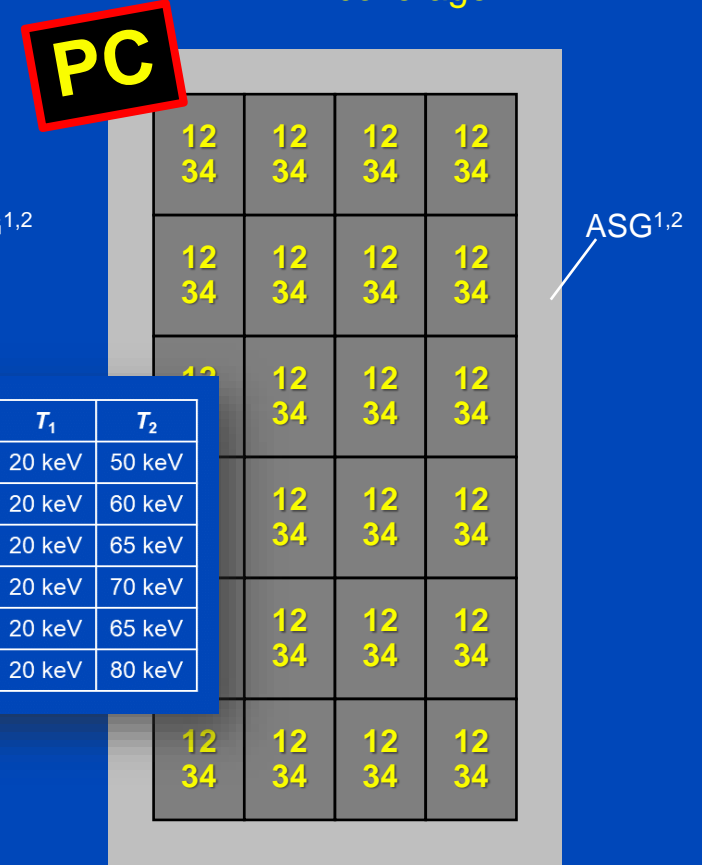
Alpha (Std, Quantum Plus)

1376 × 144 macro pixels
 pixel size 0.3 × 0.352 mm at iso
 avg. sampling 0.344 × 0.4 mm at iso
 57.6 mm z-coverage



Alpha (UHR, QuantumHD)

2752 × 120 pixels
 pixel size 0.151 × 0.176 mm at iso
 avg. sampling 0.172 × 0.2 mm at iso
 24 mm z-coverage



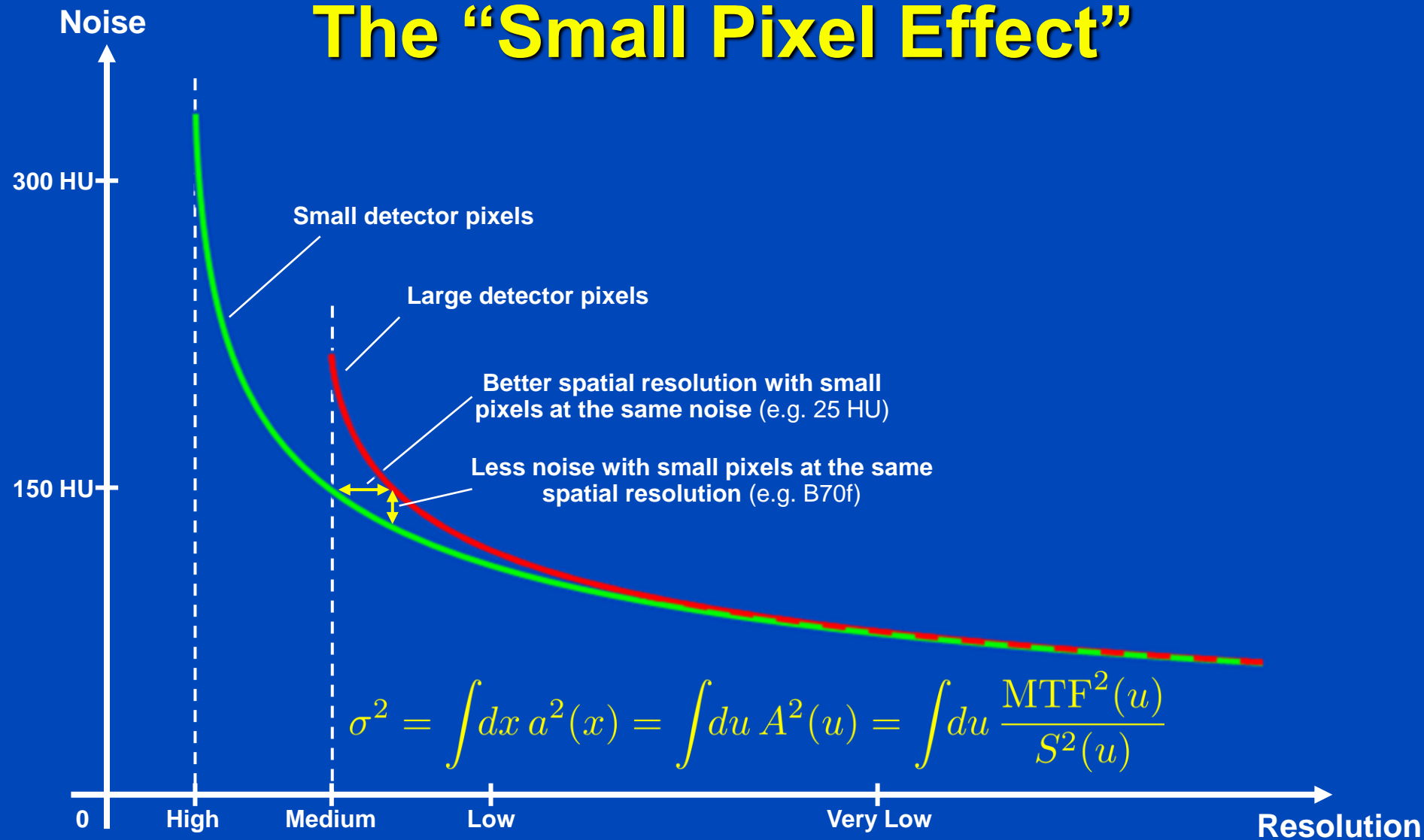
Spectrum	T ₁	T ₂
70 kV	20 keV	50 keV
90 kV	20 keV	60 keV
120 kV	20 keV	65 keV
140 kV	20 keV	70 keV
100 kV Sn	20 keV	65 keV
140 kV Sn	20 keV	80 keV

Focus sizes (Vectron): 0.181×0.226 mm, 0.271×0.7316 mm, 0.362×0.497 mm at iso
 which are 0.4×0.5 mm, 0.6×0.7 mm, 0.8×1.1 mm at focal spot

¹J. Ferda et al. Computed tomography with a full FOV photon-counting detector in a clinical setting, the first experience. European Journal of Radiology 137:109614, 2021

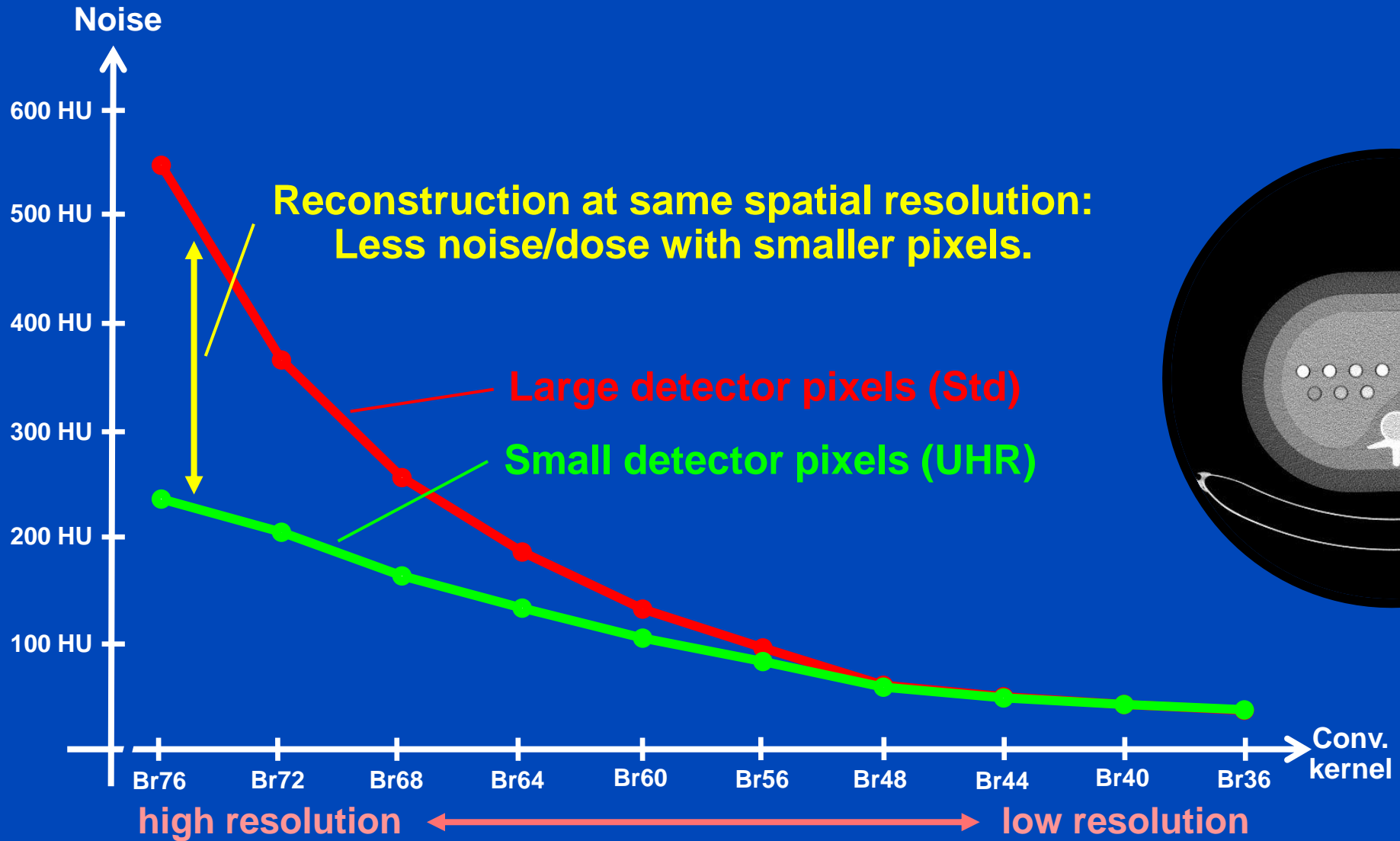
²Rajendran et al. Full field-of-view, high-resolution, photon-counting detector CT: technical assessment and initial patient experience. Phys. Med. Biol. 66:205019, 2021

The "Small Pixel Effect"



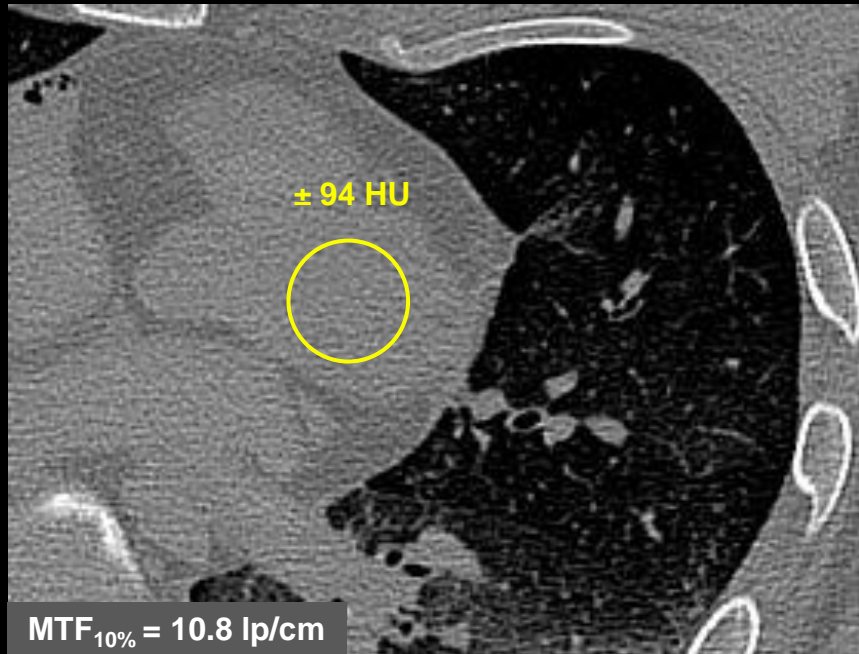
Small Pixel Effect at Naeotom Alpha

Medium Phantom, 4 mGy CTDI₃₂

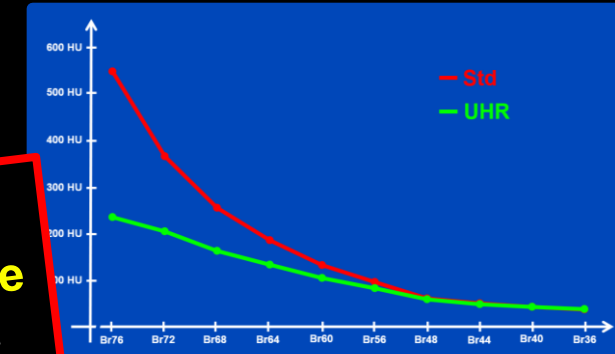
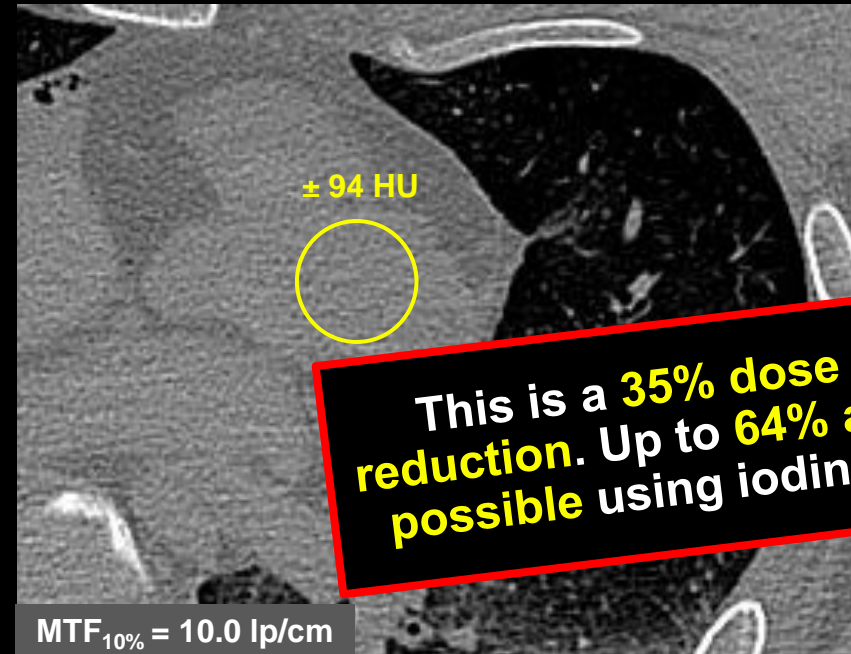


To disable the longitudinal small pixel effect, we reconstructed rather thick slices (1 mm thickness).

Energy Integrating Detector (B70f)



Photon Counting Detector (B70f)



Acquisition with EI:

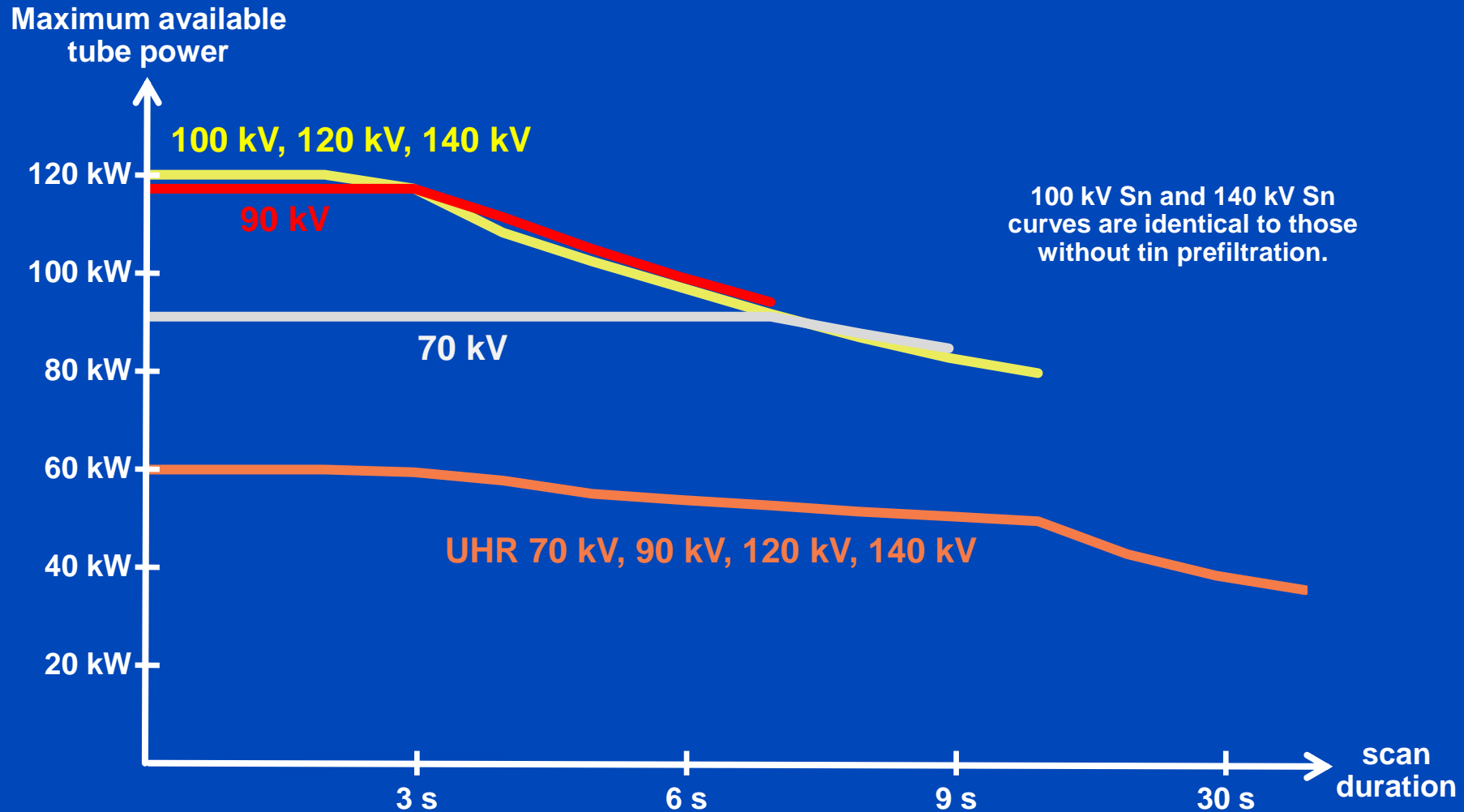
- Tube voltage of 120 kV
- Tube current of 300 mAs
- Resulting dose of $CTDI_{vol\ 32\ cm} = 22.6\ mGy$

Acquisition with UHR:

- Tube voltage of 120 kV
- Tube current of 180 mAs
- Resulting dose of $CTDI_{vol\ 32\ cm} = 14.6\ mGy$

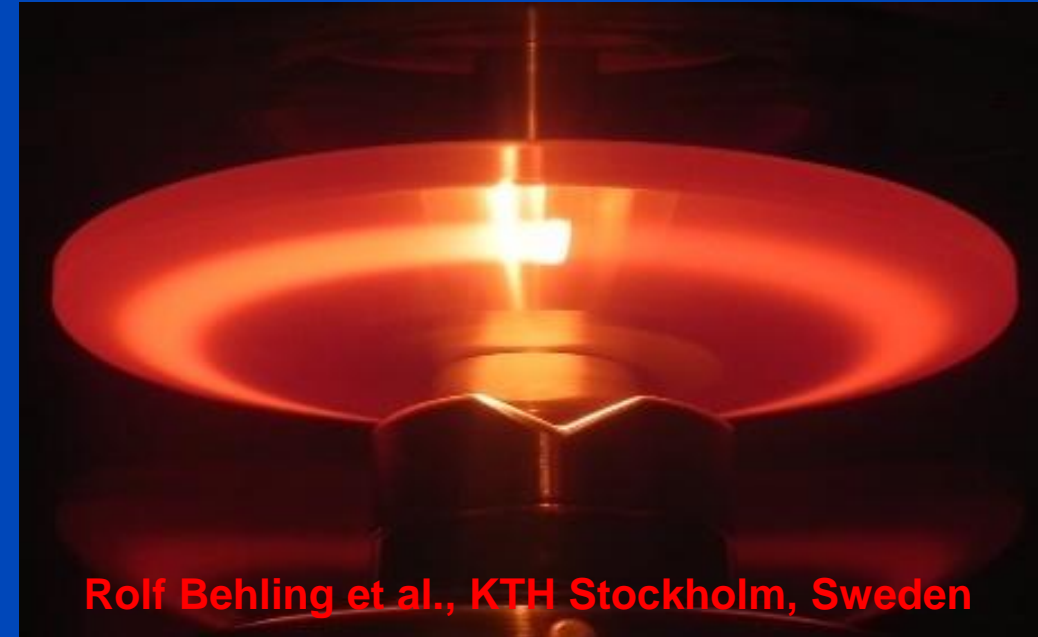
Tube Power at the Naeotom Alpha

Vectron X-Ray Tube



Conventional Target Design

- Erosion of focal spot trajectory on rotating anode target limits tube power
- Power density of focal spot is limited to below anode melting
- Problems:
 - Surface erosion
 - Excessive stress (rupture)
 - Track speed limit: about 100 m/s
 - Materials fully optimized



Patient-Specific Prefilters + Small Pixel Effect?

More X-Ray Power + More X-Ray Power

X-RAY TARGET DESIGN

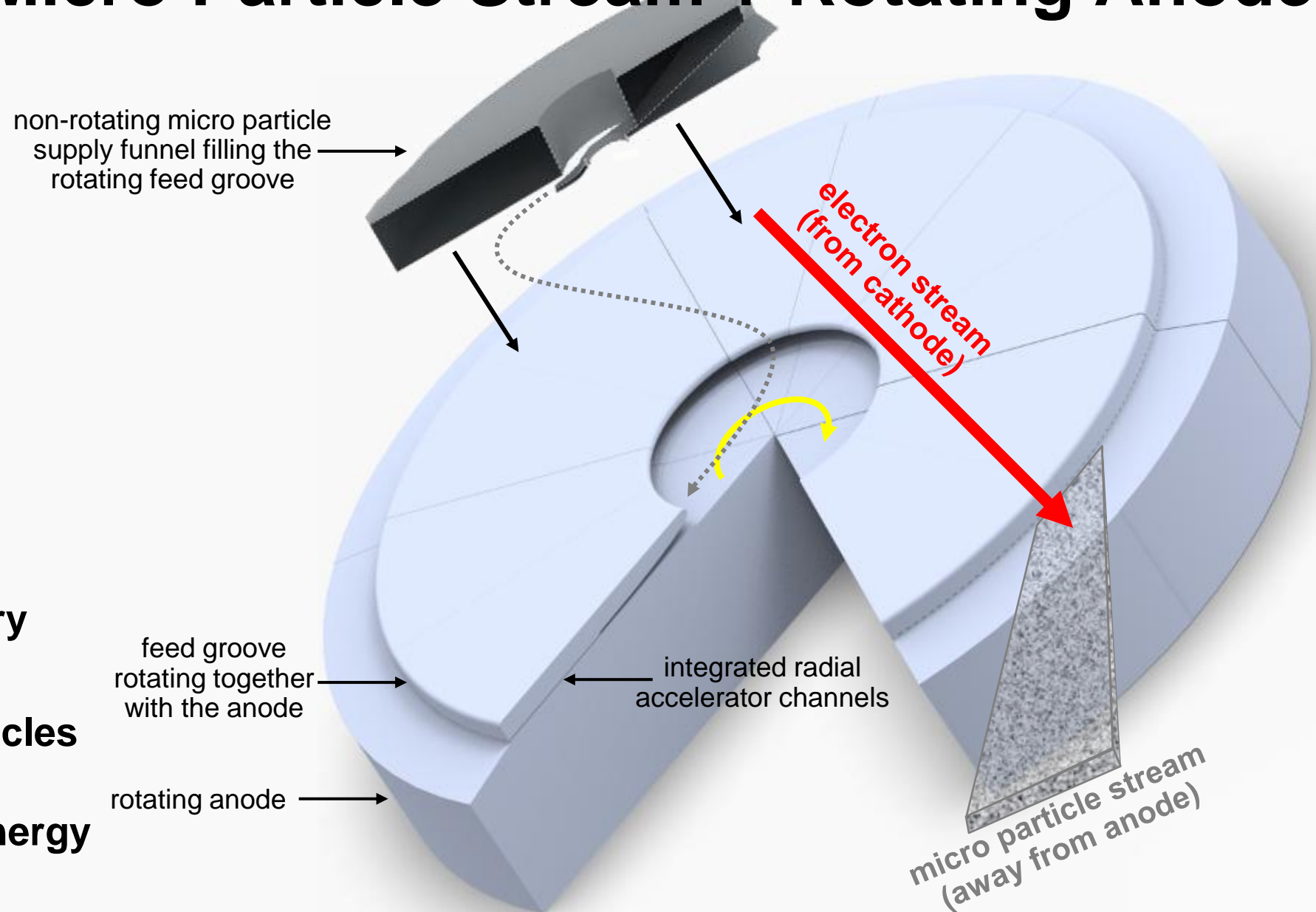
Hybrid Target: Micro Particle Stream + Rotating Anode

Micro particles pros:

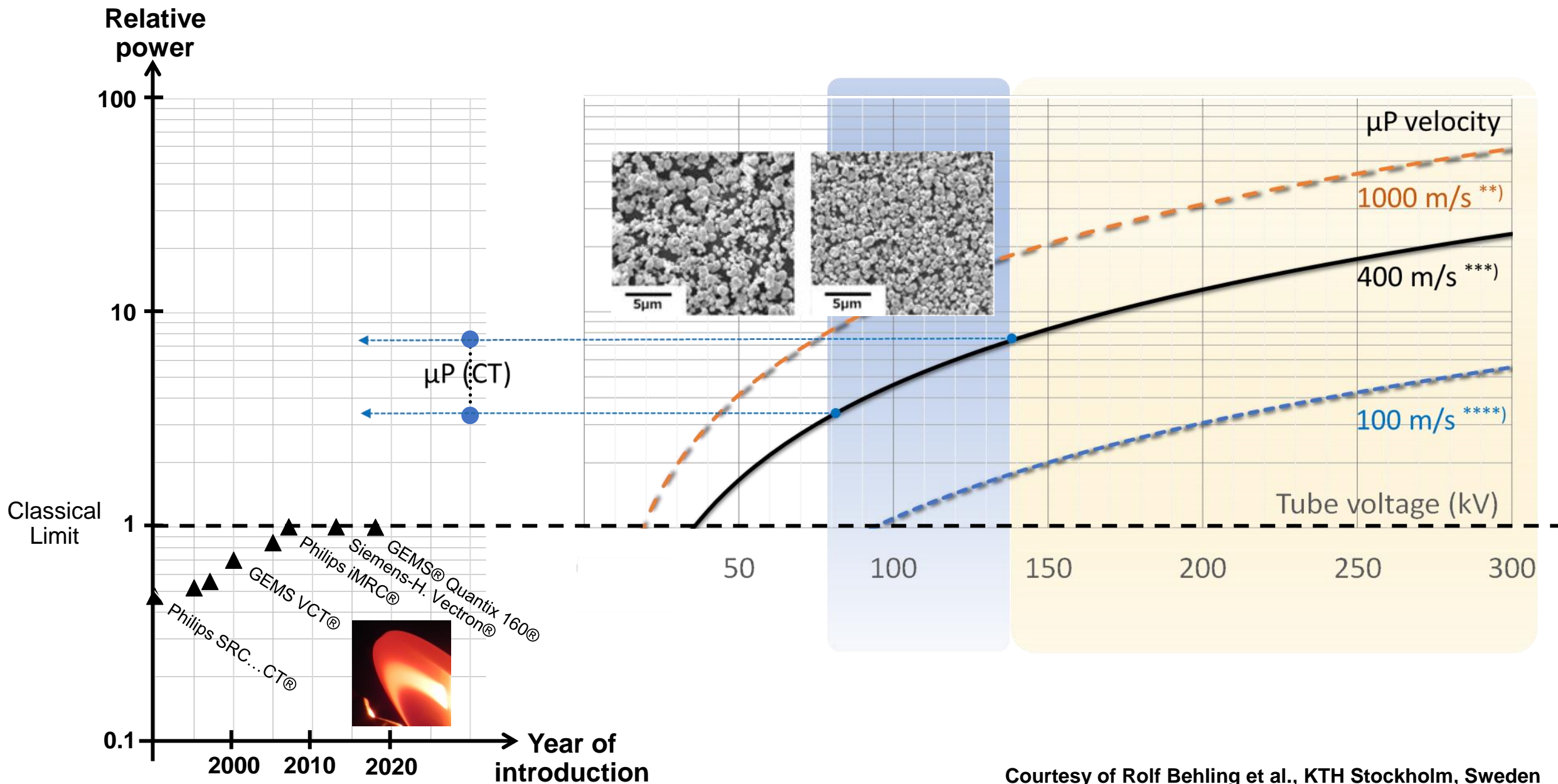
- No erosion
- 4-fold target velocity
- 3-fold heat capacity
- Remote cooling
- Full X-ray conversion possible

Micro particles challenges:

- Acceleration and recovery
- Charging of thick layers
- Separation of micro particles from insulation
- Recuperating electron energy



Gain of Power Density by Micro Particle Targets



riskTCM

RISK-MINIMIZING TUBE CURRENT MODULATION

Patient Risk-Minimizing Tube Current Modulation (riskTCM)

1. Coarse reconstruction from two scout views

- E.g. X. Ying, et al. X2CT-GAN: Reconstructing CT from biplanar x-rays with generative adversarial networks. CVPR 2019.

2. Segmentation of radiation-sensitive organs

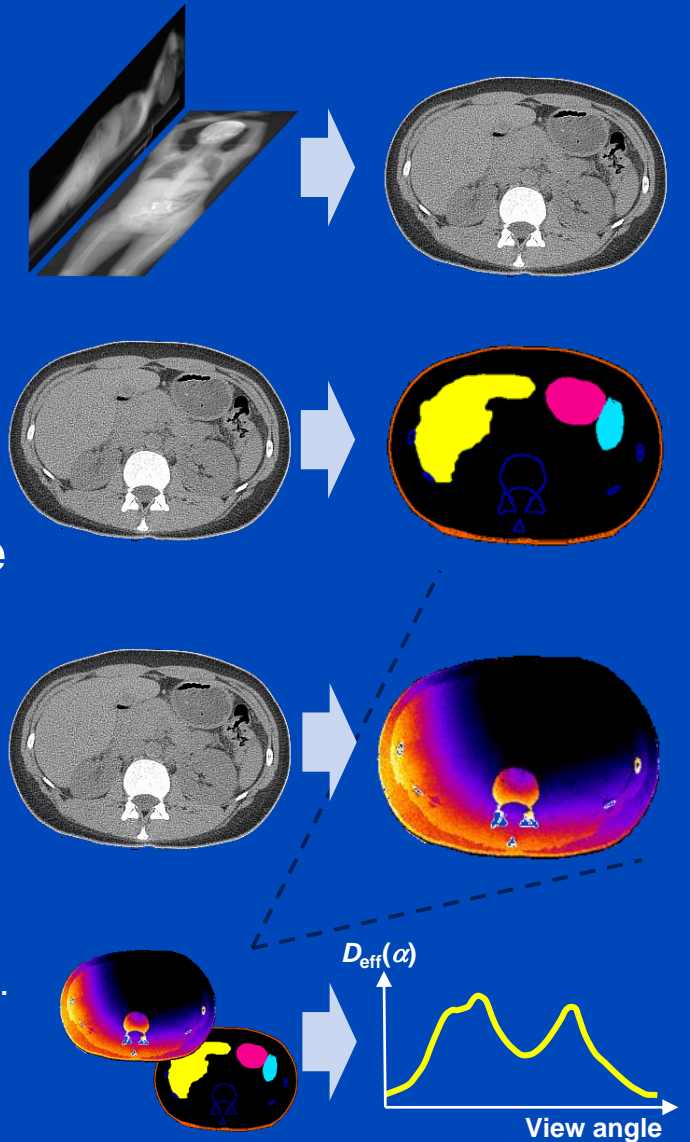
- E.g. S. Chen, M. Kachelrieß et al., Automatic multi-organ segmentation in dual-energy CT (DECT) with dedicated 3D fully convolutional DECT networks. Med. Phys. 2019.

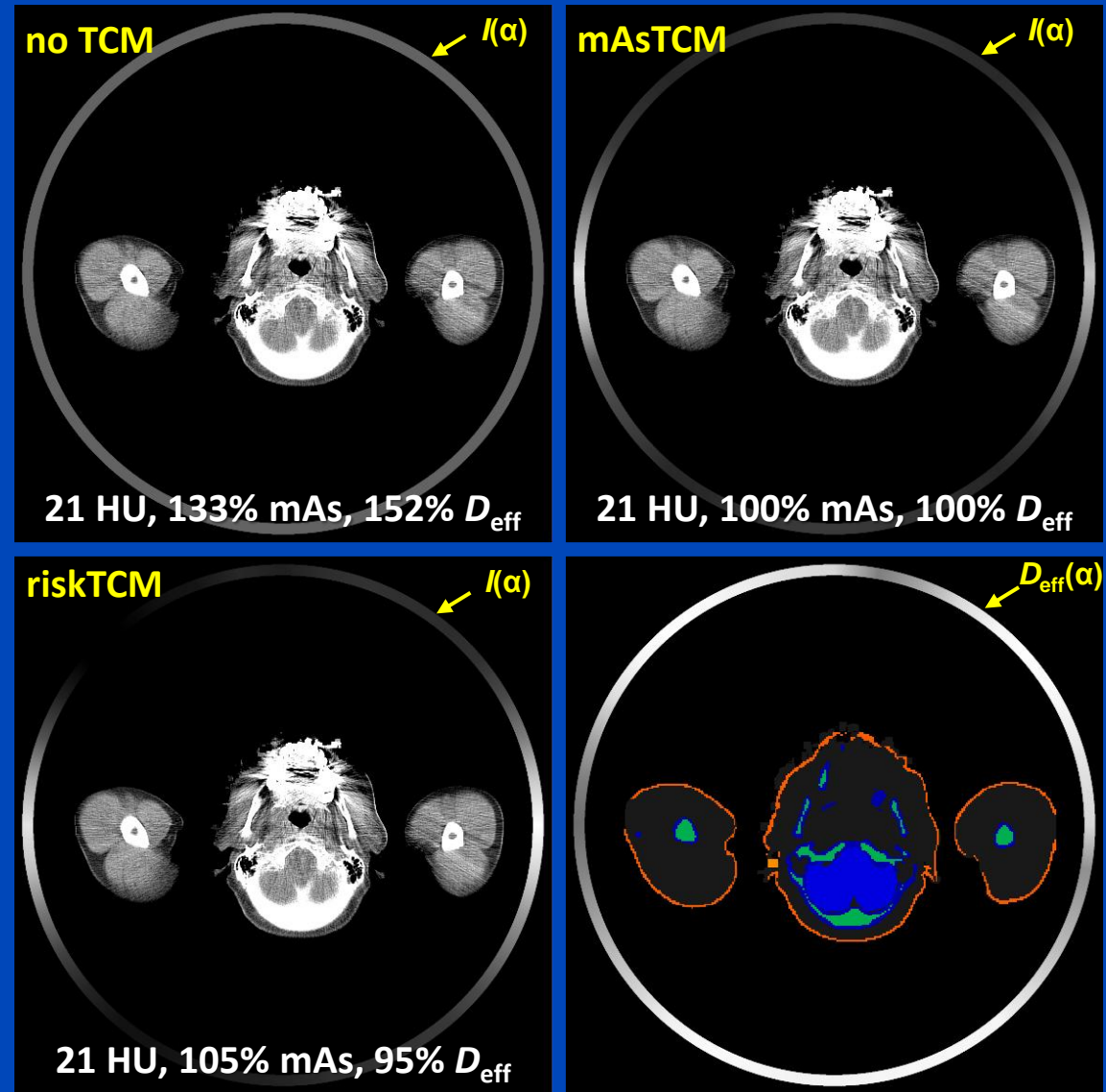
3. Calculation of the effective dose per view using the deep dose estimation (DDE)

- J. Maier, E. Eulig, S. Dorn, S. Sawall and M. Kachelrieß. Real-time patient-specific CT dose estimation using a deep convolutional neural network. IEEE Medical Imaging Conference Record, M-03-178: 3 pages, Nov. 2018.

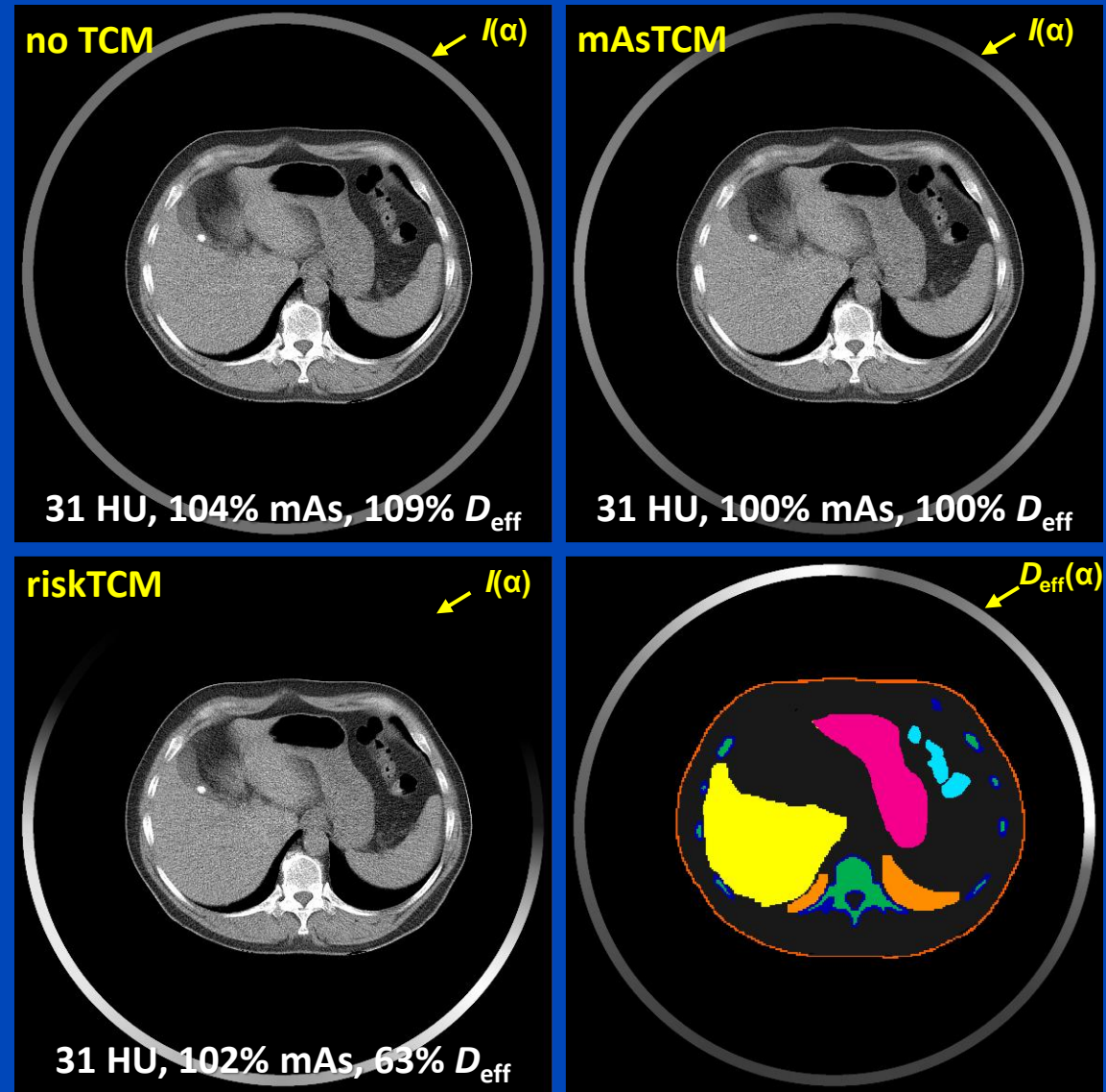
4. Determination of the tube current modulation curve that minimizes the radiation risk

- L. Klein, C. Liu, J. Steidel, L. Enzmann, M. Knaup, S. Sawall, A. Maier, M. Lell, J. Maier, and M. Kachelrieß. Patient-specific radiation risk-based tube current modulation for diagnostic CT. Med. Phys. 49(7):4391-4403, July 2022.





C = 25 HU, W = 400 HU



C = 25 HU, W = 400 HU

D_{eff} Values of riskTCM Relative to mAsTCM

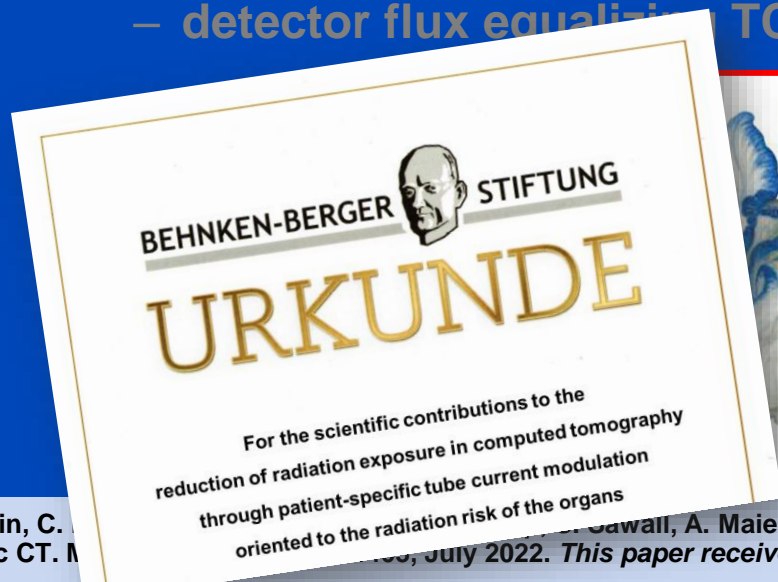
Average over all patients and across all tube voltages (70 to 150 kV)

	noTCM	mAsTCM	riskTCM
Head	110%	100%	92%
Head+Arms	162%	100%	88%
Neck	223%	100%	76%
Thorax	113%	100%	81%
Abdomen	114%	100%	71%
Pelvis	152%	100%	79%

Conclusions on riskTCM

- Risk-specific TCM minimizes the patient risk.
- With D_{eff} as a risk model riskTCM can reduce risk to 30%, compared with the gold standard.
- Other risk models, such as organ-specific, weight- and sex-specific models, can be used with riskTCM as well.
- Note:
 - mAsTCM = good for the x-ray tube
 - **riskTCM = good for the patient**
 - detector flux equalizing TCM = good for the detector

It is up to the vendors to take action!

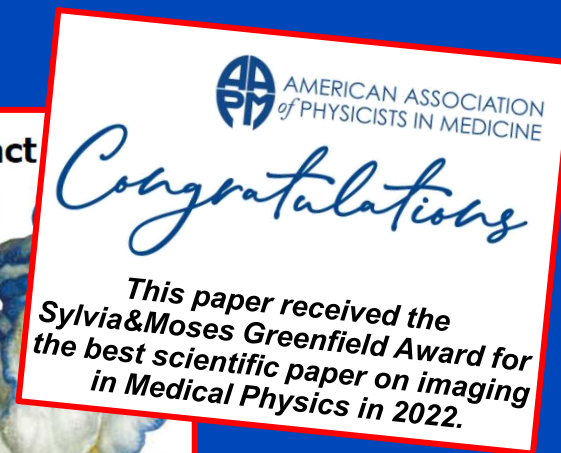


ECR 2022 – Best Research Presentation Abstract

within the topic Physics in Medical Imaging
with the presentation:

Risk-minimising tube current modulation (riskTCM) for CT – potential dose reduction across different tube voltages (16765)

L. Klein¹, C. Liu², J. Steidel¹, L. Enzmann¹, S. Sawall¹, J. Maier¹, A. Maier², M. Lell³, M. Kachelrieß¹; ¹Heidelberg/DE, ²Erlangen/DE, ³Nuremberg/DE



Thank You!



Job opportunities through marc.kachelriess@dkfz.de or through DKFZ's international PhD or Postdoctoral Fellowship programs.

Parts of the reconstruction software were provided by RayConStruct® GmbH, Nürnberg, Germany.